

MASTER COPY: PLEASE KEEP THIS "MEMORANDUM OF TRANSMITTAL" BLANK FOR REPRODUCTION PURPOSES. WHEN REPORTS ARE GENERATED UNDER THE ARO SPONSORSHIP, FORWARD A COMPLETED COPY OF THIS FORM WITH EACH REPORT SHIPMENT TO THE ARO. THIS WILL ASSURE PROPER IDENTIFICATION. NOT TO BE USED FOR INTERIM PROGRESS REPORTS; SEE PAGE 2 FOR INTERIM PROGRESS REPORT INSTRUCTIONS.

MEMORANDUM OF TRANSMITTAL

U.S. Army Research Office
ATTN: AMSRL-RO-BI (TR)
P.O. Box 12211
Research Triangle Park, NC 27709-2211

- | | |
|---|--|
| <input checked="" type="checkbox"/> Reprint (Orig + 2 copies) | <input type="checkbox"/> Technical Report (Orig + 2 copies) |
| <input type="checkbox"/> Manuscript (1 copy) | <input type="checkbox"/> Final Progress Report (Orig + 2 copies) |
| | <input type="checkbox"/> Related Materials, Abstracts, Theses (1 copy) |

CONTRACT/GRANT NUMBER: **W911NF0410224 (46637-CI-MUR)**

REPORT TITLE:

Performance of Finite-Depth Interleaved Convolutional Codes in a Rayleigh Fading Channel with Noisy Channel Estimates

Jittra Jootar, James R. Zeidler, John G. Proakis
in Proceedings of the IEEE 61st Semiannual Vehicular Technology Conference (VTC)
Stockholm, May 2005.

SUBMITTED FOR PUBLICATION TO (applicable only if report is manuscript):

Sincerely,

Dr. James Zeidler
Department of Electrical and Computer Engineering
University of California, San Diego

REPORT DOCUMENTATION PAGE

Form Approved
OMB NO. 0704-0188

Public Reporting burden for this collection of information is estimated to average 1 hour per response, including the time for reviewing instructions, searching existing data sources, gathering and maintaining the data needed, and completing and reviewing the collection of information. Send comment regarding this burden estimates or any other aspect of this collection of information, including suggestions for reducing this burden, to Washington Headquarters Services, Directorate for Information Operations and Reports, 1215 Jefferson Davis Highway, Suite 1204, Arlington, VA 22202-4302, and to the Office of Management and Budget, Paperwork Reduction Project (0704-0188), Washington, DC 20503.

1. AGENCY USE ONLY (Leave Blank)		2. REPORT DATE 1 June 2005	3. REPORT TYPE AND DATES COVERED Reprint: 01 July 2004 – 30 May 2005	
4. TITLE AND SUBTITLE Performance of Finite-Depth Interleaved Convolutional Codes in a Rayleigh Fading Channel with Noisy Channel Estimates.			5. FUNDING NUMBERS W911NF0410224	
6. AUTHOR(S) Jittra Jootar, James R. Zeidler, John G. Proakis				
7. PERFORMING ORGANIZATION NAME(S) AND ADDRESS(ES) University of California, San Diego Office of Contract & Grant Administration 9500 Gilman Dr. Mail Code 0934, La Jolla, CA, 92093-0934			8. PERFORMING ORGANIZATION REPORT NUMBER	
9. SPONSORING / MONITORING AGENCY NAME(S) AND ADDRESS(ES) U. S. Army Research Office P.O. Box 12211 Research Triangle Park, NC 27709-2211			10. SPONSORING / MONITORING AGENCY REPORT NUMBER	
11. SUPPLEMENTARY NOTES The views, opinions and/or findings contained in this report are those of the author(s) and should not be construed as an official Department of the Army position, policy or decision, unless so designated by other documentation.				
12 a. DISTRIBUTION / AVAILABILITY STATEMENT Approved for public release; distribution unlimited.			12 b. DISTRIBUTION CODE N/A	
13. ABSTRACT (Maximum 200 words) <p>In this paper, we derive the pairwise error probability of convolutional codes in a time-varying Rayleigh fading channel with finite interleaving depth and noisy channel estimates. The analysis quantifies the estimation-diversity tradeoff, which results from the opposite effects of the Doppler spread on the channel estimation accuracy and the channel diversity. It is also shown that, when the channel estimates are correct, this analysis gives the same result as an existing perfect channel estimation analysis.</p>				
14. SUBJECT TERMS N/A			15. NUMBER OF PAGES 6	
			16. PRICE CODE N/A	
17. SECURITY CLASSIFICATION OR REPORT UNCLASSIFIED	18. SECURITY CLASSIFICATION ON THIS PAGE UNCLASSIFIED	19. SECURITY CLASSIFICATION OF ABSTRACT UNCLASSIFIED	20. LIMITATION OF ABSTRACT UL	

NSN 7540-01-280-5500

Standard Form 298 (Rev.2-89)
Prescribed by ANSI Std. Z39-18
298-102

Enclosure 1

Performance of Finite-Depth Interleaved Convolutional Codes in a Rayleigh Fading Channel with Noisy Channel Estimates

Jittra Jootar, James R. Zeidler and John G. Proakis

Department of Electrical & Computer Engineering, University of California, San Diego, La Jolla, CA 92093-0407

Emails: jjootar@ucsd.edu, zeidler@ece.ucsd.edu, proakis@ece.ucsd.edu

Abstract—In this paper, we derive the pairwise error probability of convolutional codes in a time-varying Rayleigh fading channel with finite interleaving depth and noisy channel estimates. The analysis quantifies the estimation-diversity tradeoff, which results from the opposite effects of the Doppler spread on the channel estimation accuracy and the channel diversity. It is also shown that, when the channel estimates are correct, this analysis gives the same result as an existing perfect channel estimation analysis.

I. INTRODUCTION

Previous analytical studies on the performance of convolutional codes in a time-varying fading channel have focused on either imperfect channel state information (CSI) or finite-depth interleaving, while assuming the other to be perfect [1]–[3]. Since fading coefficients can be estimated with better accuracy in a slowly fading channel, a perfectly interleaved system with noisy CSI in a slowly fading channel outperforms the system in a fast fading channel. However, when the CSI is perfect but the interleaving is imperfect, due to finite interleaving depth, the performance is reversed, i.e., the system in a fast fading channel outperforms the system in a slowly fading channel [2], [3]. This is because the number of independent fading realizations available for a codeword, the number referred to as the *channel diversity* [4], of a fast fading channel is greater than that of a slowly fading channel.

In a practical system, where both CSI and interleaving are not perfect and the imperfections contribute to the performance degradation of the system, the performance analysis has to take into account both imperfections. Since small Doppler spread (slowly fading channel) is beneficial to the channel estimation accuracy but detrimental to the channel diversity, we expect to observe the estimation-diversity tradeoff as a function of the Doppler spread [4]–[6].

Because of its realistic quality and the interest in the estimation-diversity tradeoff, there has recently been growing interest in the performance analysis of coded systems with imperfect CSI and imperfect interleaving. Earlier works focused on analyzing systems with simple assumptions such as the pairwise error probability (PEP) of non-interleaved codes assuming imperfect CSI [7] or on explaining the tradeoff

observed in simulation results without a theoretical analysis [8]. An analytical result regarding the estimation-diversity tradeoff, we believed, was first presented in [6], where the authors analyzed the optimal memory lengths and the error exponent bounds for joint estimation and decoding assuming a block fading channel. The block fading assumption was also used in later works [4], [5], where the PEP for coded systems in a Rayleigh fading channel and a Rician fading channel was derived, respectively. Although block fading was assumed in many works, [9] presented an analysis without that assumption but with a more general channel model. However, the authors made an assumption that the noise components, after multiplying the received signal with the conjugate of the noisy channel estimates, can be approximated as Gaussian random variables. This assumption caused the results in [9] to be just approximated, not the exact, performance.

Although existing literature analytically described the behavior of convolutional codes with finite-depth interleaving and imperfect CSI, the analyses have been limited to specific assumptions such as block fading [4]–[6], which is not an accurate assumption for several wireless systems, or Gaussian noise component [9]. The primary focus of this paper is to derive the PEP with the assumptions that are more general and the model that incorporates implementation issues such as the choice of the pilot filter. The analytical result should consequently predict the system performance in a realistic scenario with high accuracy enabling optimizations of various design parameters. We would like to note that this analysis builds mainly upon the work on imperfect CSI by Cavers [10] and the work on non-interleaved codes with imperfect CSI by Nobelen and Taylor [7]. In addition, the mathematical model of this system is similar to the mathematical model of the correlated MRC system; thus, the method used here also resembles the ones used in [11], [12].

The paper is organized as follows. In section II, we describe the system model. Section III presents the PEP analysis. Discussions of the results and conclusions are presented in section IV and section V, respectively.

II. SYSTEM MODEL

The system considered is a convolutionally coded downlink BPSK DS-CDMA system with one transmit antenna at the

This research was supported by Core Grant No. 02-10109 sponsored by Ericsson.

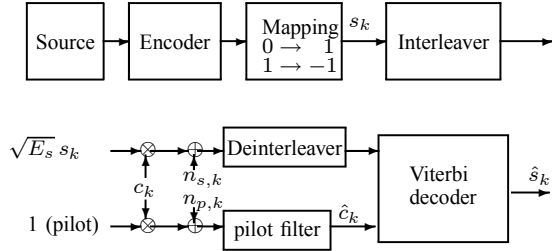


Fig. 1. System block diagram

basestation and one receive antenna at the mobile unit. The pilot channel and the data channel are transmitted simultaneously assuming that the orthogonal codes used for the pilot and the data channels have the same spreading gain resulting in the symbol period τ . The channel is assumed to be a time-varying Rayleigh fading channel. Both flat fading and frequency-selective fading channels are analyzed, but the focus is mainly on the flat fading channel. At the receiver, we assume that the pilot filter calculates the channel estimates, which are used by the Viterbi ML sequence decoder to select the most probable sequence. The pilot filter is assumed to be a $(2M + 1)$ -tap FIR filter similar to the one suggested in [10]. Note that there is no further assumption on the pilot filter coefficients, thus allowing performance comparison between different pilot filters.

The baseband representation of the system for the flat-fading channel is shown in fig. 1, where k denotes the symbol time index, s_k denotes the transmitted BPSK data, E_s denotes the data symbol energy, $n_{p,k}$ and $n_{s,k}$ denote the AWGN noise in the pilot and data channels with variances σ_p^2 and σ_s^2 , respectively. In addition, c_k denotes the fading coefficient with autocorrelation $\frac{1}{2}E[c_k c_{k-m}^*] = \sigma_c^2 R(m\tau)$ and $R(0)$ normalized to unity. Lastly, \hat{c}_k is the channel estimate, which is the output of the pilot filter.

III. PAIRWISE ERROR PROBABILITY ANALYSIS

For the rest of this paper, the following notation will be used. A lowercase bold letter denotes a column vector and an uppercase bold letter denotes a matrix. The superscripts $*$, T , H denote the complex conjugate, the matrix transpose and the matrix hermitian, respectively. The determinant of a matrix \mathbf{X} is denoted by $|\mathbf{X}|$. The square identity and the square zero matrices of size m are denoted by \mathbf{I}_m , $\mathbf{0}_m$, respectively.

Using the system model described in section II, the received pilot signal $r_{p,k}$, the received data signal $r_{s,k}$ and the channel estimate \hat{c}_k can be given by

$$r_{p,k} = c_k + n_{p,k} \quad (1)$$

$$r_{s,k} = \sqrt{E_s} s_k c_k + n_{s,k} \quad (2)$$

$$\hat{c}_k = \mathbf{h}^H \mathbf{r}_{p,k} = \sum_{m=-M}^M h_m^* r_{p,k-m}, \quad (3)$$

where $\mathbf{h} = [h_M \dots h_1 \ h_0 \ h_{-1} \dots h_{-M}]^T$ denotes the filter coefficient vector and $\mathbf{r}_{p,k} = [r_{p,k-M} \dots r_{p,k} \dots r_{p,k+M}]^T$ denotes the received pilot signal vector.

Without loss of generality, we assume that the all-zero codeword, which is mapped to an all-one BPSK sequence, is transmitted. The PEP, denoted by $P_2(d)$, which is the probability of incorrectly decoding to a codeword with the Hamming weight d can be expressed as

$$P_2(d) = \Pr(z < 0) = \int_{-\infty}^0 p_z(x) dx, \quad (4)$$

where $z = \sum_{m=1}^d Re[r_{s,g(m)} \hat{c}_{g(m)}^*]$, $p_z(x)$ denotes the probability density function (pdf) of z at x and $g(m)$, which depends on the interleaving structure and the decoded codeword, indicates the position of the post-interleaved m^{th} error symbol.

The rest of this section is organized as follows. The characteristic function of the metric z and its parameters are derived in subsection A. Subsection B explains how to calculate the PEP from the characteristic function derived in subsection A. In subsection C, we verify our analysis against the perfect CSI presented in [13]. Finally, the analysis is extended to the frequency-selective fading channel in subsection D.

A. The characteristic function

To find $P_2(d)$, we follow closely the approach suggested in [10] by recognizing that, given the transmitted codeword, z can be written in the quadratic form of correlated Gaussian random variables, i.e., $z = \mathbf{x}^H \mathbf{Q} \mathbf{x}$, where $\mathbf{x} = [r_{s,g(1)} \dots r_{s,g(d)} \ \hat{c}_{g(1)} \dots \hat{c}_{g(d)}]^T$ and

$$\mathbf{Q} = \frac{1}{2} \begin{bmatrix} \mathbf{0}_d & \mathbf{I}_d \\ \mathbf{I}_d & \mathbf{0}_d \end{bmatrix}. \quad (5)$$

The characteristic function of $\mathbf{x}^H \mathbf{Q} \mathbf{x}$ has been derived by Turin to be [14]

$$\Phi_z(s) = |\mathbf{I}_{2d} - 2s\mathbf{\Sigma}\mathbf{Q}|^{-1} = \prod_{m=1}^d (1 - s\lambda_m)^{-1}, \quad (6)$$

where $\mathbf{\Sigma}$ is the covariance matrix of \mathbf{x} and λ_m 's, for $m = 1, \dots, 2d$, denote the eigenvalues of $2\mathbf{\Sigma}\mathbf{Q}$. To determine the characteristic function of z , we only need to find the covariance matrix of \mathbf{x} . Using (1)-(3), $\mathbf{\Sigma}$ can be obtained

$$\mathbf{\Sigma} = \begin{bmatrix} \mathbf{A} & \mathbf{C} \\ \mathbf{C}^H & \mathbf{B} \end{bmatrix}$$

$$A(m_1, m_2) = E_s \sigma_c^2 R(f(m_1, m_2)\tau) + \sigma_s^2 \delta(m_1 - m_2) \quad (7)$$

$$B(m_1, m_2) = \mathbf{h}^H (\sigma_c^2 \mathbf{D}_{f(m_1, m_2)} + \sigma_p^2 \delta_{f(m_1, m_2)}) \mathbf{h}$$

$$C(m_1, m_2) = \sqrt{E_s} \sigma_c^2 \mathbf{w}_{f(m_2, m_1)}^H \mathbf{h},$$

where $f(m_1, m_2) = g(m_1) - g(m_2)$, $\delta(m)$ is the Dirac delta function, δ_e is a square matrix of size $2M + 1$ with ones on the e^{th} diagonal and zero elsewhere (command $diag([1 \dots 1], e)$ in matlab), \mathbf{D}_e is a square matrix of size $2M + 1$ with

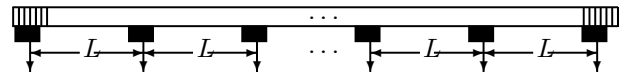


Fig. 2. The system with the interleaving depth L

$D_e(m_1, m_2) = R((e + m_1 - m_2)\tau)$ and \mathbf{w}_e is the $(M + 1)^{th}$ column of \mathbf{D}_e .

From (7), it can be seen that Σ is a function of $g(m)$. Since $g(m)$ depends on the interleaving pattern and the error codeword, the characteristic function of z and the PEP, both of which are functions of Σ , are controlled by these ‘fine’ structure of the system as well [15]. Finding the PEP for a particular interleaving pattern and error codeword is tedious and adds little insight into the overall system performance. Therefore, we will use the approximation that the interleaving depth L of a block interleaver creates the same effect as separating the d symbol errors by L symbols [2]. The illustration of this assumption is shown in fig. 2, where the black regions indicate the pilot symbols used to find the channel estimates and the downward arrows indicate the error symbols. With this approximation, Σ can be simplified by setting $g(m) = mL$, thus leading to

$$\begin{aligned} A(m_1, m_2) &= E_s \sigma_c^2 R((m_1 - m_2)L\tau) + \sigma_s^2 \delta(m_1 - m_2) \\ B(m_1, m_2) &= \mathbf{h}^H (\sigma_c^2 \mathbf{D}_{(m_1 - m_2)L} + \sigma_p^2 \delta_{(m_1 - m_2)L}) \mathbf{h} \\ C(m_1, m_2) &= \sqrt{E_s \sigma_c^2} \mathbf{w}_{(m_2 - m_1)L}^H \mathbf{h}. \end{aligned} \quad (8)$$

B. The pairwise error probability

From the definition of pdf, we know that

$$p_z(x) = \frac{1}{2\pi} \int_{-\infty}^{\infty} \Phi_z(s) e^{-sx} ds. \quad (9)$$

Substituting (9) into (4), we obtain an expression for the PEP

$$P_2(d) = \int_{\epsilon - \infty + j}^{\epsilon + \infty + j} \frac{j \Phi_z(s)}{2\pi s} ds = -\text{Res} \left[\frac{\Phi_z(s)}{s} \text{ at LHP poles} \right], \quad (10)$$

where $\text{Res}[f(s) \text{ at } a]$ denotes the residue of $f(s)$ at $s = a$, and the residue can be calculated by

$$\text{Res}[f(s) \text{ at } a] = \lim_{s \rightarrow a} \frac{p^{(v-1)}(s)}{(v-1)!}, \quad (11)$$

where $p(s) = (s - a)^v f(s)$, $p^{(v)}(s)$ denotes the v^{th} derivative of $p(s)$ and v is the order of the pole at a .

Alternatively, $P_2(d)$ can be found numerically via the Gauss-Chebyshev approximation [16],

$$P_2(d) \approx \frac{1}{2N} \sum_{m=1}^N \left(\text{Re}[\Phi_z(\varrho_m)] + \tau_m \text{Im}[\Phi_z(\varrho_m)] \right), \quad (12)$$

where $\varrho_m = \epsilon(1 + j\tau_m)$, $\tau_m = \tan((2m - 1)\pi/2N)$, ϵ lies between the left half-plane poles and the imaginary axis, and, in general, N between 32 and 64 is sufficient [16].

C. The perfect channel estimates

The performance of finite-depth interleaved convolutional codes in a time-varying fading channel assuming perfect CSI is well-known. In this subsection, we will verify that in the limit when there is no error in the channel estimates, our analysis provides the same result as the perfect CSI analysis presented in [13].

First, let us consider the analysis from [13]. The characteristic function of the instantaneous data SNR γ is

$$\Phi_\gamma(s) = |\mathbf{I}_d - s\bar{\gamma}\mathbf{K}|^{-1}, \quad (13)$$

where $\bar{\gamma} = E_s \sigma_c^2 / \sigma_s^2$ is the average data SNR, which is also referred to as the data E_b/N_o , and \mathbf{K} is a square matrix of size d with $K(m_1, m_2) = R((m_1 - m_2)L\tau)$. Substituting the alternative form of the complementary error function [17]

$$\text{erfc}(x) = \frac{2}{\pi} \int_0^\infty \frac{e^{-x^2(t^2+1)}}{t^2+1} dt \quad \text{for } x > 0, \quad (14)$$

into the average PEP expression

$$P_2(d) = \int_0^\infty Q(\sqrt{2\gamma}) p(\gamma) d\gamma, \quad (15)$$

the average PEP becomes

$$P_2(d) = \frac{1}{\pi} \int_0^\infty \int_0^\infty \frac{e^{-\gamma(t^2+1)}}{t^2+1} p(\gamma) d\gamma dt \quad (16)$$

$$= \frac{1}{\pi} \int_0^\infty \frac{\Phi_\gamma(jv)|_{jv=-(t^2+1)}}{t^2+1} dt \quad (17)$$

$$= \frac{1}{\pi} \int_0^\infty \frac{1}{t^2+1} \prod_{m=1}^d (1 + \tilde{\lambda}_m \bar{\gamma} (1 + t^2))^{-1} dt, \quad (18)$$

where $\{\tilde{\lambda}_1, \dots, \tilde{\lambda}_d\}$ are the eigenvalues of \mathbf{K} and $2Q(x) = \text{erfc}(x/\sqrt{2})$.

Second, let us now consider the analysis presented in this paper. The perfect CSI assumption can be realized by setting $\sigma_p^2 = 0$, $M = 1$ and $\mathbf{h} = [1]$, leading to

$$2\Sigma\mathbf{Q} = \begin{bmatrix} \sqrt{E_s} \sigma_c^2 \mathbf{K} & E_s \sigma_c^2 \mathbf{K} + \sigma_s^2 \mathbf{I}_d \\ \sigma_c^2 \mathbf{K} & \sqrt{E_s} \sigma_c^2 \mathbf{K} \end{bmatrix}. \quad (19)$$

After some math, it can be shown that the eigenvalues of $2\Sigma\mathbf{Q}$, $\{\lambda_1, \dots, \lambda_{2d}\}$, are functions of the eigenvalues of \mathbf{K} , i.e.,

$$\lambda_{2m-1}, \lambda_{2m} = \sqrt{E_s} \sigma_c^2 \tilde{\lambda}_m \left(1 \pm \sqrt{1 + \sigma_s^2 / E_s \sigma_c^2 \tilde{\lambda}_m} \right). \quad (20)$$

Since $P_2(d)$ is invariant to the scaling of the poles or the eigenvalues [18], $\lambda_m / \sigma_c^2 \sqrt{E_s}$ can replace λ_m in (6) to find $P_2(d)$. Using the scaled eigenvalues $\lambda_m / \sigma_c^2 \sqrt{E_s}$ in (6) and (10) with the relationship (20), we obtain

$$\begin{aligned} P_2(d) &= \frac{j}{2\pi} \int_{\epsilon - j\infty}^{\epsilon + j\infty} \frac{1}{s} \prod_{m=1}^d \left(1 - 2s\tilde{\lambda}_m - \frac{\tilde{\lambda}_m s^2}{\bar{\gamma}} \right)^{-1} ds \quad (21) \\ &= \frac{1}{\pi} \int_0^\infty \frac{1}{y^2 + 1} \prod_{m=1}^d \left(1 + \tilde{\lambda}_m \bar{\gamma} (1 + y^2) \right)^{-1} dy, \quad (22) \end{aligned}$$

where (22) results from replacing s and ϵ in (21) with $\bar{\gamma}(jy - 1)$ and $-\bar{\gamma}$, respectively. We would like to point out that, since \mathbf{K} is positive definite, the eigenvalues $\{\tilde{\lambda}_1, \dots, \tilde{\lambda}_d\}$ are positive. Thus, the negative poles in (21) are $-\bar{\gamma} - \sqrt{\bar{\gamma}^2 + \bar{\gamma}/\tilde{\lambda}_m}$ for $m = 1, \dots, d$ and setting $\epsilon = -\bar{\gamma}$ satisfies the condition for ϵ stated in section III-B.

Comparing (18) and (22), it is clearly seen that the two equations are identical. Thus, we can conclude that our result is equal to the result in [13] under the perfect CSI assumption.

D. Frequency-selective fading

When the frequency-selective fading channel is considered, we assume that each path fades independently with no self-noise, which is the result from sufficiently large spreading gains and spreading codes with good correlation properties [19]. The autocorrelation of the l^{th} path is assumed to be $\frac{1}{2}E[c_k^l c_{k-m}^{l*}] = \sigma_{c,l}^2 R_l(m\tau)$, and for a fair comparison between the flat fading and the frequency-selective fading, we also assume that the total received energy for the frequency-selective fading channel is equal to the total received energy for the flat fading channel, i.e., $\sum_{l=1}^{\mathcal{L}} \sigma_{c,l}^2 = \sigma_c^2$, where \mathcal{L} is the number of resolvable paths.

Using the same approach used in previous subsections, it can be shown that the characteristic function of the metric z for the frequency-selective fading channel is basically the multiplication of the characteristic function of z_l corresponding to the l^{th} path, i.e.,

$$\Phi_z(s) = \prod_{l=1}^{\mathcal{L}} |\mathbf{I}_{2d} - 2s \Sigma_l \mathbf{Q}|^{-1} \quad (23)$$

with

$$\begin{aligned} \Sigma_l &= \begin{bmatrix} \mathbf{A}_l & \mathbf{C}_l \\ \mathbf{C}_l^H & \mathbf{B}_l \end{bmatrix} \\ A_l(m_1, m_2) &= E_s \sigma_{c,l}^2 R_l(f(m_1, m_2)\tau) + \sigma_s^2 \delta(m_1 - m_2) \\ B_l(m_1, m_2) &= \mathbf{h}_l^H (\sigma_{c,l}^2 \mathbf{D}_f(m_1, m_2) + \sigma_p^2 \delta_{f(m_1, m_2)}) \mathbf{h}_l \\ C_l(m_1, m_2) &= \sqrt{E_s} \sigma_{c,l} \mathbf{w}_{f(m_2, m_1), l}^H \mathbf{h}_l. \end{aligned} \quad (24)$$

We would like to note that, although no self-noise assumption is made, the analysis can easily be extended to account for the self-noise by treating the self-noise as an additional Gaussian noise component [19].

IV. RESULTS

In this section, we will discuss analytical results calculated by the Gauss-Chebyshev approximation. Unless specified otherwise, the following values are used: $E_s = 1$, $\sigma_s^2 = 0.1$, $\sigma_c^2 = 0.5$, $\sigma_p^2 = 10$, $d = 18$, $1/\tau = 30$ KHz, $f_c = 2$ GHz, $R(m) = J_0(2\pi f_d \tau)$ (Jakes model [20]). The pilot filter is assumed to be an 11-tap Wiener filter with

$$\mathbf{h} = (\sigma_c^2 \mathbf{D}_0 + \sigma_p^2 \mathbf{I}_{(2M+1)})^{-1} \sigma_c^2 \mathbf{w}_0. \quad (25)$$

Also note that d , f_c , and τ are chosen to agree with the 12.2kbps test specification for WCDMA [21].

A. The effect of $f_d \tau$ and pilot E_p/N_o

An illustration of the estimation-diversity tradeoff is presented in fig. 3. In this figure, the PEP curves of convolutionally coded systems with $L = 30$ in slowly and fast fading channels as functions of the pilot E_p/N_o are compared, where the pilot E_p/N_o , or the pilot SNR, is equal to σ_c^2/σ_p^2 . The normalized Doppler spread $f_d \tau$ corresponding to the slowly and the fast fading channels are assumed to be 0.01 and 0.1, respectively.

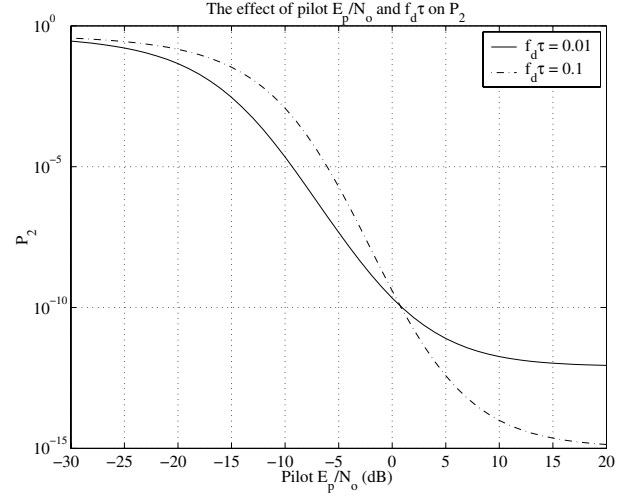


Fig. 3. The effect of the pilot E_p/N_o and $f_d \tau$ on P_2

We can see that when the pilot E_p/N_o is very small (-30 dB), the performance of the system with small Doppler spread (system A) and the performance of the system with large Doppler spread (system B) are almost equal with system A being slightly better. As the pilot E_p/N_o increases, the performance difference increases until the pilot E_p/N_o reaches -10 dB, and then it decreases and eventually reverses such that system B outperforms system A when the pilot E_p/N_o is large. The reason for this behavior can be explained as follows. At small pilot E_p/N_o , the accuracy of CSI dominates the performance [6] causing system A, which can better estimate the fading coefficients due to larger channel memory, to perform better; thus, the performance difference increases as the pilot E_p/N_o increases. But as the pilot E_p/N_o increases further, system B also gains better CSI accuracy and eventually achieves the accuracy close to that of system A. Therefore, when the pilot E_p/N_o increases pass a certain value (-10 dB for this particular example), system B, which has larger channel diversity, begins to catch up with system A and eventually outperforms system A.

We would like to note that, although the system behavior is well understood, values such as the range of the pilot E_p/N_o that system A outperforms system B and vice versa are not trivial. An analysis such as the one presented herein is needed to quantify these values.

B. Improving the performance through the interleaving depth

In addition to the Doppler spread, the channel diversity can also be increased by increasing the interleaving depth L , which, unlike the Doppler spread, is a controllable parameter limited only by the allowable delay of the system. In fig. 4, we illustrate the effect of L on the performance for $f_d \tau = 0.005$ and 0.0005. Large L significantly improves the performance at large pilot E_p/N_o but not as much at small pilot E_p/N_o . The reason is the same as the one stated in subsection A that the accuracy of CSI, not the channel diversity, dominates the

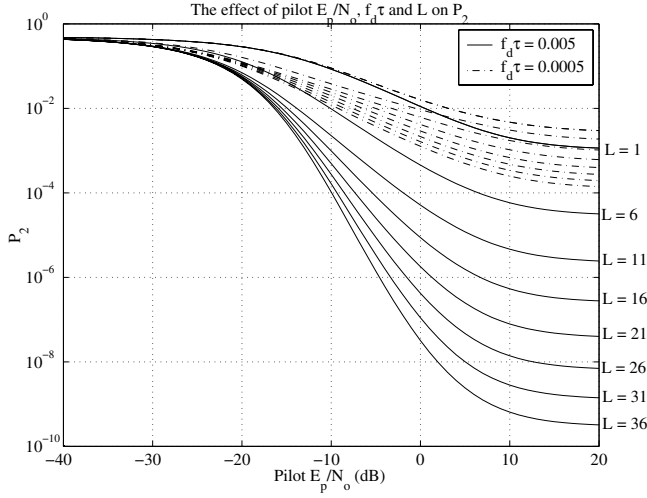


Fig. 4. The effect of pilot E_p/N_o , $f_d\tau$ and L on P_2

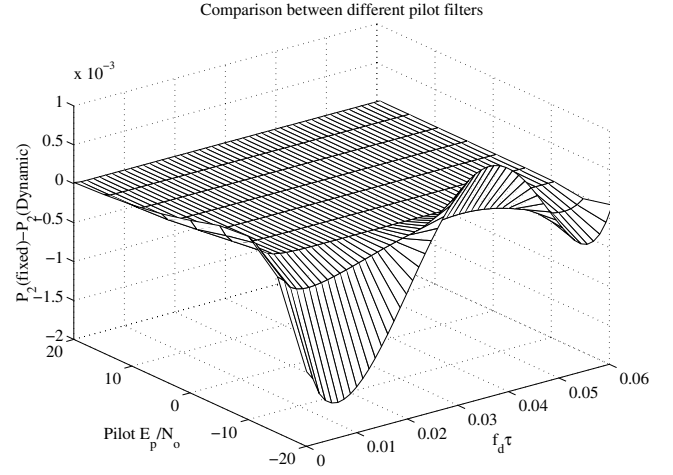


Fig. 6. The effect of \mathbf{h}

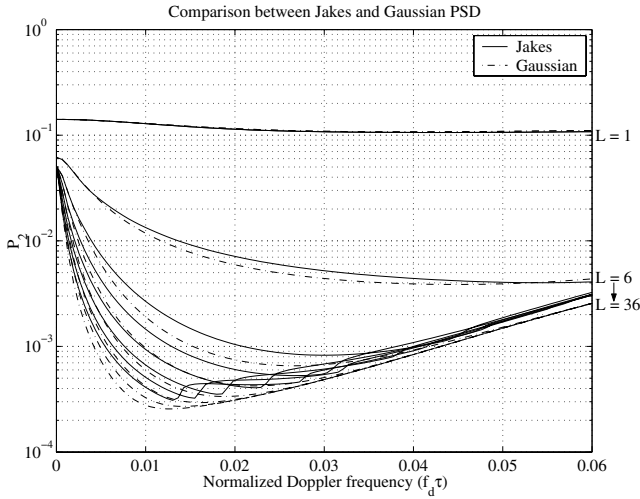


Fig. 5. Gaussian and Jakes PSD

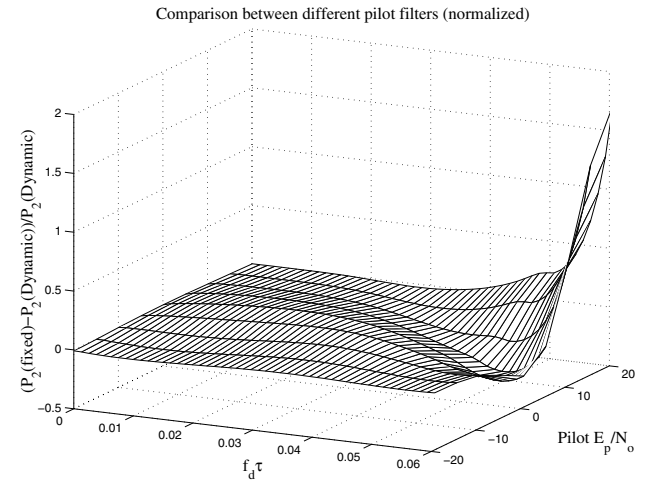


Fig. 7. The effect of \mathbf{h} (normalized)

performance at small pilot E_p/N_o [6]. We can also observe diminishing performance improvement from increasing L as L gets larger. This behavior is the result of diminishing return from diversity gain as it approaches infinity.

C. The optimal $f_d\tau$

It was suggested in [6] that the estimation-diversity tradeoff can be observed in the optimal $f_d\tau$, the Doppler spread that is small enough for the channel estimator to make good channel estimates but large enough to gain reasonable channel diversity. In fig. 5, we illustrate the optimal $f_d\tau$ corresponding to various interleaving depths for channels with the Jakes power spectral density (PSD) and the Gaussian PSD.

The optimal $f_d\tau$'s are clearly seen in the plot, and the optimal $f_d\tau$ corresponding to a large L is smaller than the one corresponding to a smaller L . We also observe a significant difference between different PSD's that there are

oscillations in the curves corresponding to the Jakes PSD but none for the Gaussian PSD. This is because the autocorrelation function corresponding to the Jakes PSD, which is the zero-order Bessel function of the first kind, is not monotonically decreasing, unlike the Gaussian autocorrelation corresponding to the Gaussian PSD.

D. Filter choice

Up until now, we have used the *dynamic* Wiener filter calculated according to the system's pilot E_p/N_o and $f_d\tau$ as the pilot filter. In order to do this, the receiver must have the knowledge of the pilot E_p/N_o and $f_d\tau$ of the system. In a real system, this knowledge may not be available or it may not be accurate. Thus, instead of using a dynamic filter, which changes the filter tap coefficients according to the system condition, a simple receiver may use a *static* filter, which never changes its filter tap coefficients. In fig. 6 - 7,

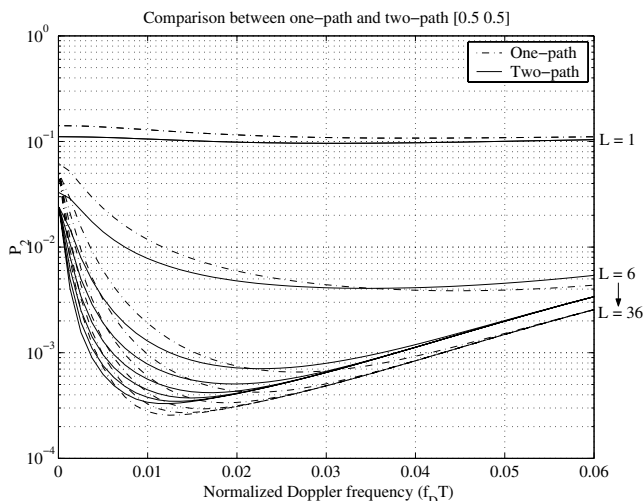


Fig. 8. The effect of multi-path

we compare the performance of the two filters where the fixed filter is randomly chosen to be the Wiener filter corresponding to the pilot $E_p/N_o = -10$ dB and $f_d\tau = 0.0482$.

In fig. 6, the z-axis represents $P_2(\text{fixed}) - P_2(\text{dynamic})$, the value which is positive when the dynamic filter outperforms the fixed filter. We can see from this plot that the dynamic filter is sometimes outperformed by the fixed filter. This behavior is expected because the optimal receiver, which gives the smallest PEP, is the joint estimation-decoding; thus, using the optimal estimator and the optimal decoder does not guarantee the optimal result. In fig. 7, the normalized version of fig. 6 is shown where the z-axis represents $(P_2(\text{fixed}) - P_2(\text{dynamic}))/P_2(\text{dynamic})$ indicating the impact of the filter choice experienced by the system. It is clear that the filter choice is critical when the pilot E_p/N_o and $f_d\tau$ are large.

E. The frequency-selective fading channel

Fig. 8 shows the PEP when the system is in a frequency-selective fading channel assuming that there are two resolvable paths and each has half of the average power of the path in the flat fading case. Path diversity added by multi-path causes the performance of the frequency-selective fading to be better than the flat fading when $f_d\tau$ is small. But, due to smaller pilot E_p/N_o per path, the channel estimation accuracy of the frequency-selective fading deteriorates much faster as $f_d\tau$ increases, leading to worse performance at large $f_d\tau$.

V. CONCLUSIONS

In this paper, we have analytically derived the pairwise error probability for systems with finite-depth interleaved convolutional codes with noisy channel estimates, providing insight into a realistic system performance. Various system behaviors were discussed, i.e., the optimal channel memory, the sensitivity to the interleaving depth and the sensitivity to the pilot filter choice.

For a sanity check, we have also proved that, when there is no error in the channel estimates, the analytical results

from our analysis agree with the existing results from the perfect channel state information analysis. In addition, we have extended the flat fading analysis to a more general frequency-selective fading analysis and showed that, although the frequency-selective fading increase the path diversity, the smaller pilot E_p/N_o per path causes the system to be outperformed by the flat fading when the Doppler spread is large.

REFERENCES

- [1] L. Chong and L. Milstein, "Convolutionally coded multicarrier DS-CDMA with imperfect channel estimation," in *Proc. 39th Allerton Conf. Communications, Control, Computing*, pp. 543–552, Oct. 2001.
- [2] F. Gagnon and D. Haccoun, "Bound on the error performance of coding for nonindependent Rician-fading channels," *IEEE Trans. Commun.*, vol. 40, pp. 351–360, Feb. 1992.
- [3] G. Kaplan and S. Shamai, "Achievable performance over the correlated Rician channel," *IEEE Trans. Commun.*, vol. 42, pp. 2967–2978, Nov. 1994.
- [4] S. A. Zummo and W. E. Stark, "Performance analysis of binary coded systems over Rician block fading channels," in *Proc. IEEE MILCOM'03*, pp. 314–319, Oct. 2003.
- [5] S. A. Zummo and W. E. Stark, "Performance analysis of coded systems over block fading channels," in *Proc. IEEE VTC Fall 2002*, pp. 1129–1133, Sept. 2002.
- [6] A. P. Worthen and W. E. Stark, *On the channel memory-diversity tradeoff in communication systems*. In Information, coding and mathematics Kluwer Academic Publishers, 2002.
- [7] R. V. Nobelen and D. P. Taylor, "Analysis of the pairwise error probability of noninterleaved codes on the Rayleigh-fading channel," *IEEE Trans. Commun.*, vol. 44, pp. 456–463, Apr. 1996.
- [8] W. K. M. Ahmed and P. J. McLane, "Random coding error exponents for flat fading channels with realistic channel estimation," *IEEE J. Select. Areas Commun.*, vol. 18, pp. 369–379, Mar. 2000.
- [9] J. Lai and N. B. Mandayam, "Performance analysis of convolutionally coded DS-CDMA systems with spatial and temporal channel correlations," *IEEE Trans. Commun.*, vol. 51, pp. 1984–1990, Dec. 2003.
- [10] J. K. Cavers, "An analysis of pilot symbol assisted modulation for Rayleigh fading channels," *IEEE Trans. Veh. Technol.*, vol. 40, pp. 686–693, Nov. 1991.
- [11] F. A. Dietrich and W. Utschick, "Maximal ratio combining of correlated Rayleigh fading channels with imperfect channel knowledge," *IEEE Commun. Lett.*, vol. 7, pp. 419–421, Sept. 2003.
- [12] P. Shamaian and L. B. Milstein, "Effect of mutual coupling and correlated fading on receive diversity systems using compact antenna arrays and noisy channel estimates," in *Proc. IEEE Globecom'03*, pp. 1669–1673, Dec. 2003.
- [13] J. Luo, J. R. Zeidler, and J. G. Proakis, "Coded error performance of MIMO systems in frequency selective Nakagami fading channels," in *Proc. IEEE International Conference on Communications (ICC'02)*, pp. 1959–1963, Apr. 2002.
- [14] G. L. Turin, "The characteristic function of hermitian quadratic forms in complex normal variables," *Biometrika*, vol. 47, pp. 199–201, June 1960.
- [15] M. Rice and E. Perrins, "A simple figure of merit for evaluating interleaver depth for the land-mobile satellite channel," *IEEE Trans. Commun.*, vol. 49, pp. 1343–1353, Aug. 2001.
- [16] E. Biglieri, G. Caire, G. Taricco, and J. Ventura-Traveset, "Simple method for evaluating error probabilities," *Electronic Letters*, vol. 32, pp. 191–192, Feb. 1996.
- [17] M. Abramovitz and I. A. Stegun, *Handbook of mathematical functions*. New York: Dover, 1972.
- [18] J. Jootar, J. R. Zeidler, and J. G. Proakis, "Performance of alamouti space-time code in time-varying channels with noisy channel estimates," in *Proc. Wireless Communications and Networking Conf.*, Mar. 2005.
- [19] J. G. Proakis, *Digital Communications*. New York: McGraw-Hill.
- [20] W. C. Jakes, *Microwave Mobile Communications*. New Jersey: IEEE Press, 1994.
- [21] 3GPP, "Technical specification group radio access network, physical channels and mapping of transport channels onto physical channels, 25.211."